ACS OMEGA

Open Access

http://pubs.acs.org/journal/acsodf

Article

Utilizing Silk Sericin as a Biomaterial for Drug Encapsulation in a Hydrogel Matrix with Polycaprolactone: Formulation and Evaluation of Antibacterial Activity

Dona Deb,[§] Bably Khatun,[§] Bidyarani Devi M, Mojibur R. Khan, Neelotpal Sen Sarma, and Kamatchi Sankaranarayanan*

Cite This: *ACS Omega* 2024, 9, 32706−32716

Read Online

ACCESS | Metrics & More | Article Recommendations

ABSTRACT: Hydrogels have emerged as a potential tool for enhancing bioavailability and regulating the controlled release of therapeutic agents. Owing to its excellent biocompatibility, silk sericin-based hydrogels have garnered interest in biomedical applications. This study focuses on synthesizing a soft hydrogel by blending silk sericin (SS) and polycaprolactone (PCL) at room temperature. The physicochemical characteristics of the hydrogels have been estimated by different analytical techniques such as UV−visible spectroscopy, Fourier transform infrared spectroscopy (FTIR), X-ray diffraction (XRD), and scanning electron microscopy (SEM). The rheological studies demonstrate the non-Newtonian behavior of the hydrogels. Further, the porosity analysis indicates a commendable absorption capacity of the hydrogels. The swelling degree of the hydrogels has been checked in both distilled water and buffer solutions of different pHs (2−10). Moreover, the drug release profile of the hydrogels, using diclofenac sodium (DS) as a model drug, has revealed a substantial release of approximately 67% within the first 130 min with a drug encapsulation efficiency of 60.32%. Moreover, both the empty and the drug-loaded hydrogels have shown antibacterial properties against Gram-positive and Gram-negative bacteria, with the drug-loaded hydrogels displaying enhanced effectiveness. Additionally, the prepared hydrogels are biodegradable, demonstrating their future prospects in biomedical applications.

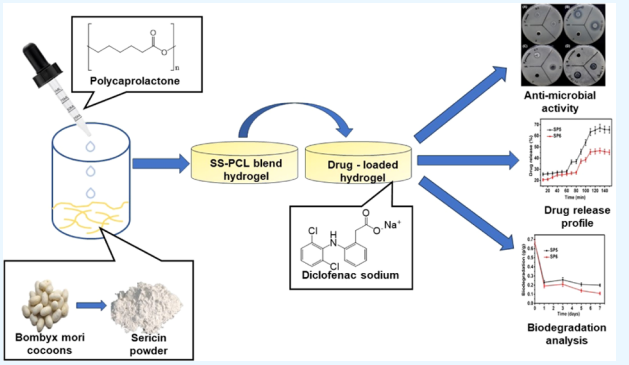

1. INTRODUCTION

A drug delivery system involves diverse physicochemical methods to regulate the release of drugs, increasing their therapeutic effectiveness and reducing side effects.[1] Conventional drug delivery systems have several disadvantages such as poor drug bioavailability, premature metabolism of drugs, nonspecific targets, poor patient compliance, and many more.[2] Releasing drugs in a controlled fashion can minimize their toxicity, elevate site concentration, and improve patient response.[3] Encapsulation of drugs within polymer matrices, such as microemulsions, lipid vesicles, and hydrogel systems, enables precise drug release.[4] Among the various drug encapsulation matrices, hydrogels are soft, three-dimensional polymeric materials characterized mainly by their water-swelling properties.[5] Their versatile nature makes them applicable in various fields, such as electronics, agriculture, and medicine.[6] Both natural and synthetic polymers are employed for the synthesis of hydrogels.[7]

Silk, a natural polymer, comprises two different proteins: sericin and fibroin.[8] Silk fibroin is hydrophobic, while sericin is a hydrophilic adhesive protein.[9] Both sericin and fibroin have been explored to synthesize hydrogels intended for drug delivery.[10] Sericin is obtained as a byproduct during the degumming of silk cocoons.[11] It comprises 18 amino acids featuring hydroxyl, carbonyl, and amino groups in their side chains.[12] Sericin's functional groups facilitate the interlink, amalgamation, and copolymerization with other polymers, resulting in biomaterials with improved properties.[13] Sericin exhibits antioxidant, anti-inflammatory, and antibacterial activities.[14] However, sericin alone is unsuitable for creating hydrogels due to its amorphous nature and weak mechanical properties.[15−17] Hence, cross-linking of sericin is the need of the hour to improve its properties for its use in drug delivery applications.[18] Chemical cross-linking agents such as dialdehyde

Received: March 13, 2024
Revised: May 21, 2024
Accepted: May 29, 2024
Published: July 16, 2024

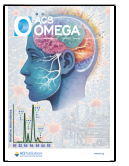

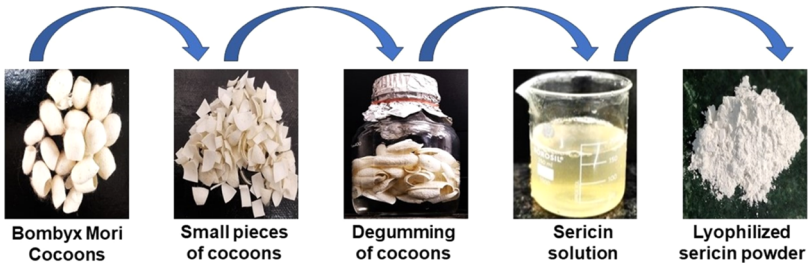

Figure 1. Schematic representation of sericin isolation.

starch, glutaraldehyde, and formaldehyde involve toxicity risks, emphasizing the importance of physical cross-linking by blending natural and synthetic polymers.[19] Physically cross-linked hydrogels are formed by molecular entanglements and/or secondary forces including ionic, H-bonding, or hydrophobic forces[20] and can further modulate their properties such as mechanical strength, and can be used for controlled drug delivery systems.[21,22] FDA-approved synthetic polymers such as poly(vinyl alcohol) (PVA), polycaprolactone (PCL), and poly(vinylpyrrolidone) (PVP) can be employed for physical cross-linking with silk sericin.[23] In this study, we have used PCL with silk sericin as it is reported to be compatible with antibiotics and nonsteroidal anti-inflammatory drugs (NSAIDs) and has been used in sustained-release systems.[24] Its hydrophobic nature facilitates the uniform distribution of hydrophobic drugs within the support matrix, further enhancing its versatility in medical applications.[25] Various biomedical applications of PCL are bone engineering tissue engineering/repair, wound healing scaffolds, drug delivery, and many more.[26]

Gang Tao et al. developed an SS/PVA hydrogel for wound dressing, demonstrating its efficacy in accelerating tissue restoration, angiogenesis, and collagen deposition to foster wound healing.[27] Zhao et al. devised an SS/PLLA scaffold, establishing its effectiveness as a wound dressing material.[28] Ekasurya et al. crafted an SS/PVA hydrogel specifically for diabetic foot ulcer treatment, showcasing its capability to regenerate skin tissue.[29] Tuancharoensri et al. engineered an SS/PHEMA hydrogel scaffold for tissue engineering, offering insights into tailoring hydrogel properties for potential use in skin tissue regeneration within tissue engineering contexts.[30] Critical literature review on the development of sericin-based hydrogels was conducted by different aspects such as type and nature of cross-linker, natural and synthetic polymers used in literature, mode of fabrication of hydrogels, and their different properties that are studied. To date, to our knowledge, PCL is novel for blending with sericin to study the controlled drug delivery system.

Uncontrolled release of most of the drugs used for disease treatment can cause potential health-related issues.[31−34] Diclofenac sodium (DS), an NSAID, is the sodium form of *o*-(2,6-dichlorophenylamino)-phenyl acetic acid, which helps in treating ankylosing spondylitis, rheumatoid arthritis, and osteoarthritis because of its fever-reducing, pain-relieving, and anti-inflammatory properties.[35−37] However, its uncontrolled delivery can lead to peptic ulcers and gastrointestinal bleeding, and controlled delivery of DS can mitigate these adverse effects.[38]

Herein, we report the development of hydrogels by combining SS and PCL for the controlled release of DS. The physicochemical properties of the formed hydrogels have been validated by different bioanalytical methods. Various concentrations of SS and PCL have been combined to obtain a suitable mechanical strength for optimal drug release. Additionally, the antibacterial activity and biodegradability studies of the prepared hydrogels have been done for their suitability in biomedical applications.

2. EXPERIMENTAL SECTION

2.1. Materials. *Bombyx mori* silk cocoons were purchased from a local market and used as a source of sericin. Polycaprolactone (PCL) with $M_W \sim 14\,000$ g/mol and $M_N \sim 10\,000$ g/mol was purchased from Sigma-Aldrich. Sodium dihydrogen phosphate, disodium hydrogen phosphate, sodium hydroxide, and hydrochloric acid (∼35%) were obtained from Merck, Germany. All other chemicals were of analytical grade and used without further purification.

2.2. Isolation of Sericin. A high-temperature and high-pressure (HTHP) degumming method was employed to extract sericin, a protein found in silk.[39,40] Briefly, cocoons were cut into small fragments, washed thoroughly with double distilled water to remove dirt, and dried at room temperature for 2−3 days. The cocoons were then immersed in double distilled water with a ratio of 1:30 (grams of cocoons:mL of water) and then heated to 120 °C for 30 min in an autoclave (Autoclave ES-315). The mixture was cooled to room temperature, centrifuged (Eppendorf Centrifuge 5920 Ri), and filtered to remove the remaining fibroin fibers. The obtained sericin solution was lyophilized (catalogue no.: 710612070, LABCONCO) to get a sericin powder. The schematic representation of sericin isolation is shown in Figure 1.

2.3. Ratio Optimization of SS to PCL for Hydrogel Formation. Hydrogels of SS and PCL were prepared by simple blending at room temperature without using any cross-linkers. 1% (w/v) SS and 1% (w/v) PCL solutions were prepared separately in distilled water and acetic acid, respectively. The PCL solution was prepared by incorporating PCL granules into glacial acetic acid and placing them in a sonicator (Sonicator LMUC-3) for 30 min for complete dissolution of the polymer. Finally, the PCL solution was diluted in water to obtain a concentration of 1% (v/v) and neutralized with phosphate buffer solution (PBS) at pH 7.4. SS and PCL solutions were mixed in different volume ratios such as 1:1, 2:1, 3:1, 4:1, 5:1, 6:1, 1:2, 1:3, 2:3, 5:2, and 7:2 under stirring conditions at room temperature for 30 min to form different hydrogels, which were coded as SP1, SP2, SP3, SP4, SP5, SP6, SP7, SP8, SP9, SP10, and SP11. The SS/PCL solutions were then left undisturbed to form hydrogels. The resulting hydrogels were kept in a refrigerator to avoid any contamination.

2.4. Preparation of Drug-Loaded SS/PCL Hydrogel. Two different ratios (5:1 and 6:1) of SS and PCL were chosen for preparing the diclofenac sodium (DS)-loaded SS/PCL hydrogel based on the optimized ratio of SS and PCL.

https://doi.org/10.1021/acsomega.4c02453
ACS Omega 2024, 9, 32706−32716

Diclofenac sodium is a poorly water-soluble drug[41] and highly soluble in organic solvents such as ethanol, DMSO, and dimethylformamide.[42,43] So, the ethanolic solution of DS was added to 1% (w/v) SS solution and left under stirring at 70 °C until ethanol evaporated.[44] 1% (v/v) PCL solution was then added, stirred, and left undisturbed to form the hydrogel.

2.5. UV−Visible Spectroscopy. UV−visible spectra of the hydrogel samples in transmission mode were taken using a UV−visible spectrophotometer (SHIMADZU UV-2600) in the 800−200 nm wavelength range. The blank measurements were taken without samples.

2.6. Fourier Transform Infrared Spectroscopy. PerkinElmer Spectrum 2 FTIR spectrophotometer was used to record the IR spectra of the lyophilized hydrogel samples using a diamond crystal in total reflection mode in the wavenumber range of 4000−400 cm^{-1}.

2.7. X-ray Diffraction Analysis. An X-ray diffraction (XRD) study was conducted to assess the crystallinity of the lyophilized hydrogel samples. The diffractogram patterns of the samples were examined using a Bruker D8 advanced diffractometer equipped with a Cu Kα radiation source, employing a locked-couple X-ray diffraction technique.

2.8. Scanning Electron Microscopy. Field emission scanning electron microscopy (FESEM) was employed to investigate the morphological characteristics of the hydrogel samples. The lyophilized hydrogel samples were coated with a gold−palladium layer and then subjected to FESEM imaging using a Zeiss SIGMA VP-FESEM electron microscope, operating at 5 kV with a working distance of 3−5 mm.

2.9. Rheological Study. The rheological experiments were performed using an Anton Paar MCR-92 Rheometer with a cone plate (D-CP/PP7) at 25 °C. The results have been presented using four parameters: viscosity, shear storage modulus (G'), shear loss modulus (G''), and tan δ, which provide information on elasticity and viscous characteristics.

2.10. Porosity. The porosity of the prepared hydrogel samples was evaluated by the solvent displacement method. For this, a predetermined volume of hydrogels was filled in a dialysis membrane pouch and preweighed before submerging in ethanol for 24 h. After 24 h, the pouches were removed, excess ethanol was wiped with filter paper, and then the weight of hydrogel-containing pouches was measured. The porosity percentage can be calculated by the following equation:[4545]

$$\text{porosity}(\%) = \frac{M_2 - M_1}{\rho V} \times 100$$

where M_2 and M_1 are the weights of hydrogel samples after and before submerging in ethanol, respectively. V is the volume of hydrogel samples, and ρ is the density of ethanol. The presented data are the mean ± SD of at least three measurements per sample.

2.11. Swelling Experiments. The swelling behavior of hydrogels was checked in both distilled water and buffer solutions. For this, hydrogels were filled in a dialysis membrane pouch and were preweighed before submerging in distilled water and buffer solution of pHs 2, 4, 6, 8, and 10. At predetermined time intervals, pouches were removed, excess water and buffer solutions were wiped with filter paper, and then the weight of hydrogel-containing pouches was taken. The swelling percentage was calculated using the following equation:[4646]

$$\text{swelling}(\%) = \frac{W_s - W_d}{W_d} \times 100$$

where W_d is the weight of dry gel and W_s is the weight of swollen gel. This procedure was repeated for triplicate samples.

2.12. *In Vitro* Drug Encapsulation Efficiency (DEE). To determine the drug encapsulation efficiency (DEE), predetermined weights of hydrogel samples were immersed in PBS solution having pH 7.4 for 24 h. After 24 h, it was stirred for 15 min and filtered. After adequate dissolution, the drug content in the filtrate was analyzed using a UV−visible spectrophotometer (SHIMADZU UV-2600) at 535 nm. DEE was calculated by the following equation:[4747]

$$\text{DEE}(\%) = \frac{\text{actual drug content}}{\text{theoretical drug content}} \times 100$$

This procedure was repeated for triplicate samples.

2.13. In Vitro Drug Release Profile. The drug-loaded hydrogels were put separately into two different dialysis membrane pouches, placed in two different beakers containing 100 mL of PBS solution each, and left at 37 °C. At intervals of 10 min for 3 h, 5 mL aliquots of this solution were withdrawn, and an equivalent amount of fresh PBS solution was added to maintain the total volume of 100 mL. The absorbance of each sample was measured at 535 nm using a UV−visible spectrophotometer (SHIMADZU UV-2600) to determine the percentage of drug released. This procedure was repeated for triplicate samples.

2.14. Drug Release Kinetics. The release kinetics of diclofenac sodium from the prepared hydrogels was studied using four different mathematical models, i.e., zero-order,[48] pseudo-first-order,[49] Korsmeyer−Peppas law,[50] and Higuchi square root law.[51] The mathematical expressions of these models are shown below:

$$\text{zero order } M_t = M_0 + k_0 t$$

$$\text{pseudo first order } \log(M_e - M_t) = \frac{-k_1}{2.303t} + \log M_e$$

$$\text{Korsmeyer−Peppas law } F = \frac{M_t}{M_e} = Kt^n$$

$$\text{Higuchi square root law } M_t = k_2 t^{1/2}$$

where F is the fractional swelling ratio, M_t and M_e are the drug release at different time t and equilibrium conditions respectively, and K, k_0, k_1, and k_2 are the rate constants.

2.15. In Vitro Antibacterial Analysis. To determine the antibacterial potential of the drug-loaded and without drug-loaded hydrogels, the previously described well diffusion method[52] was used following Clinical & Laboratory Standards Institute (CLSI) Guidelines[53] of two pathogens *Staphylococcus aureus* (Gram-positive) and *Klebsiella pneumoniae* (Gram-negative). To maintain sterile conditions, the necessary materials were autoclaved at 121 °C for 20 min. Both pathogens were cultured overnight at 37 °C in Nutrient Broth. The pathogens were collected in the exponential phase and incorporated with soft agar (2×10^9 CFU (colony forming unit)/mL) and let solidify for 15−20 min. The solidified agar was then punctured with an 8 mm diameter gel puncher. The hydrogels were then introduced into the holes, and the agar plates were incubated at 37 °C. After 24 h, the zone of inhibition was recorded.

2.16. In Vitro Biodegradation Analysis. For the in vitro biodegradation investigation, a phosphate buffer (PBS) solution (pH 7.4) was prepared, and the hydrogel samples were

https://doi.org/10.1021/acsomega.4c02453
ACS Omega 2024, 9, 32706−32716

immersed in that solution at 37 °C under gentle stirring conditions. At predetermined intervals (1, 3, 5, and 7 days), the PBS solution was removed, the samples were superficially cleaned with blotting paper, and their weights were recorded. The extent of biodegradation was determined using the following equation:[54,54]

$$D = \frac{W_i - W_t}{W_i}$$

where W_i and W_t are the initial weight and the weight of the sample degraded at an arbitrary time, respectively. This procedure was repeated for triplicate samples.

2.17. Statistical Analysis. Antibacterial activities by the hydrogels against two different pathogens were analyzed using one-way analysis of variance (ANOVA) within SigmaPlot software, and the data were expressed as the mean ± standard error mean. The differences in the values were considered statistically significant at $P \leq 0.05$. The significance of the samples against two different pathogens is displayed in Figure 8E,F, respectively, as *** ($P \leq .001$) and NS as nonsignificant.

3. RESULTS AND DISCUSSION

3.1. Ratio Optimization. We first evaluated the formation of a stable hydrogel by optimizing various concentrations of SS and PCL as summarized in Table 1. The hydrogel formation after 15 min of incubation is depicted in Figure 2. It can be observed that in the case of SP5 and SP6, where SS and PCL were mixed in the ratios of 5:1 and 6:1, the hydrogel formed was stable compared with all of the other concentrations. Moreover, only SS can also form hydrogel after 3 h of incubation, as shown in Figure 2. The pH values of the formed hydrogels are 5.89 for SP5 and 6.02 for SP6. These hydrogels can be taken forward for transdermal drug delivery application because the pH of our skin is 5.0−6.0.[55−57] Transdermal delivery of a drug is a noninvasive alternative to the oral route.[58] It eliminates gastric irritation, prevents hepatic first-pass metabolism, prevents gastric degradation of the drug, provides sustained release of the drug, is noninvasive, and improves patient compliance.[59]

Table 1. Ratio Optimization of the Hydrogels

hydrogel code	SS to PCL volume ratio	gel formation (yes/no)
SS	1:0	yes
SP1	1:1	no
SP2	2:1	no
SP3	3:1	no
SP4	4:1	no
SP5	5:1	yes
SP6	6:1	yes
SP7	1:2	no
SP8	1:3	no
SP9	2:3	no
SP10	5:2	no
SP11	7:2	no

3.2. UV−Vis Spectroscopy. The percentage transmittance of SS, SP5, and SP6 was checked using UV−visible spectroscopy, as shown in Figure 3. Although it is not apparent from the digital photo, visually, it was observed that the color of SS changed from transparent yellowish-white to completely white (SP5 and SP6) with the addition of PCL. The gradual loss of transparency to complete opacity can be examined from the UV−visible spectra, in which there is a change in wavelengths from ≈300−320 to ≈350−380 nm, indicating a poor visible light barrier. It can also be observed that SP5 has a marginally lower visible light barrier than SP6. As a result, we can conclude that SP5 is a more stable hydrogel with better blending compared with SP6.[60]

3.3. Fourier Transform Infrared Spectroscopy. FTIR spectroscopy was done better to understand the molecular interactions of the SS-PCL hydrogel blend and is shown in Figure 4a. In SS, two peaks were observed at 1540 and 1640 cm^{-1}, respectively, corresponding to the amide II group (N−H bending and C−N stretching) and the amide I group (C═O stretching).[61] Further, the peak at 1640 cm^{-1} represents the formation of β-sheet structures.[62] In SP5 and SP6, two sharp peaks were observed at 1524 and 1620 cm^{-1}, respectively, representing the interaction of the N−H group of sericin and the C═O group of polycaprolactone. These results demonstrate the possibility of forming an amide bond between sericin and polycaprolactone.[63] However, the peaks observed at 1068, 1403, and 1246 cm^{-1} correspond to the amide II and amide III groups, respectively, in both hydrogels.[64] The presence of amide III groups in both hydrogels suggests that the cross-linking process might induce a minor transformation from random coil structure to β-turn.[65]

3.4. X-ray Diffraction Analysis. The XRD pattern of pure sericin hydrogel and the prepared hydrogel blended with PCL is displayed in Figure 4b. Pure sericin hydrogel (SS) showed three peaks at diffraction angles of 22.1, 43.4, and 63.6°, respectively. At these diffraction angles, SP5 and SP6 showed broader peaks than SS, which could be due to the formation of interlinked structures in SP5 and SP6 compared with SS.[66,67] These results indicate the formation of stable hydrogels of SS and PCL.

3.5. Scanning Electron Microscopy. The surface morphology of the hydrogel samples can be determined from SEM analysis, as portrayed in Figure 4c. SP5 showed porous structures compared with SP6. Such porous structures could be of greater use as injectable hydrogels for biomedical applications.[68]

3.6. Rheological Study. Flow curves represent the response of a material to steady shear flow, which provides insights into its

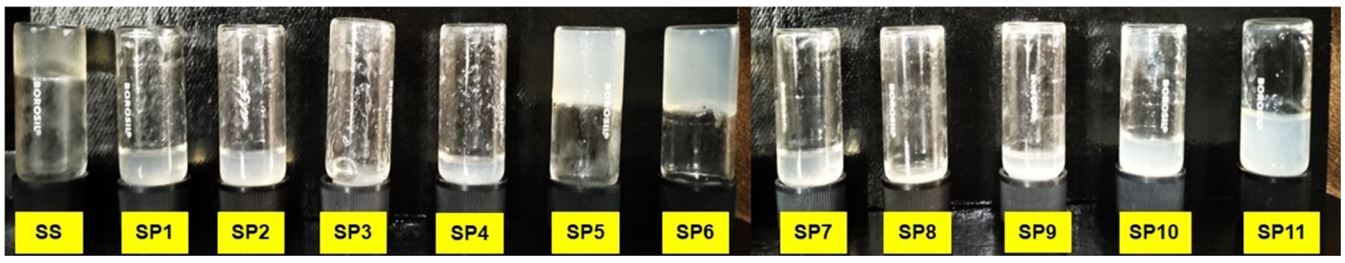

Figure 2. Hydrogel formation after 15 min of incubation.

https://doi.org/10.1021/acsomega.4c02453
ACS Omega 2024, 9, 32706−32716

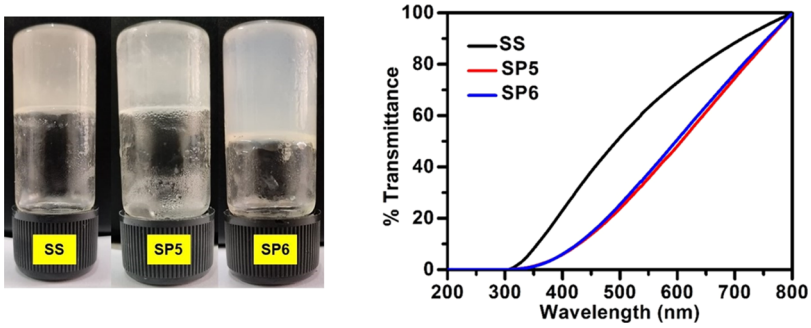

Figure 3. Digital photograph and UV−visible transmittance spectra of hydrogel samples.

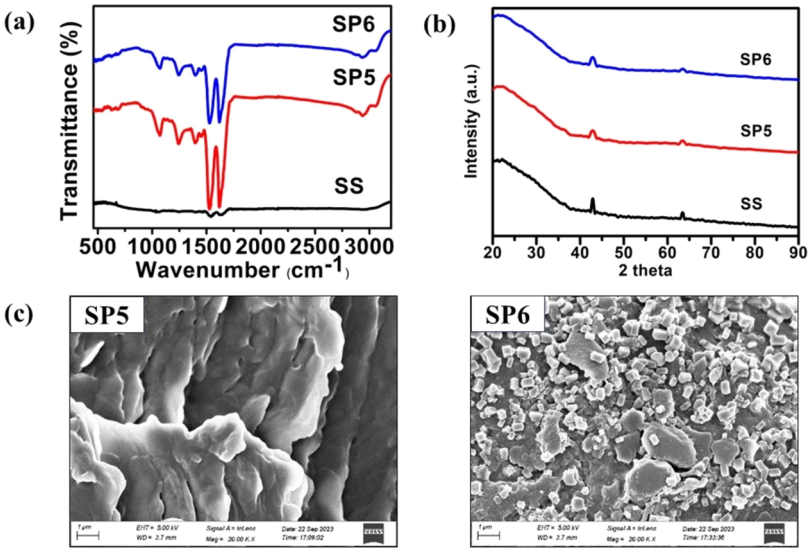

Figure 4. (a) FTIR spectra, (b) the XRD pattern, and (c) SEM images of the hydrogel samples.

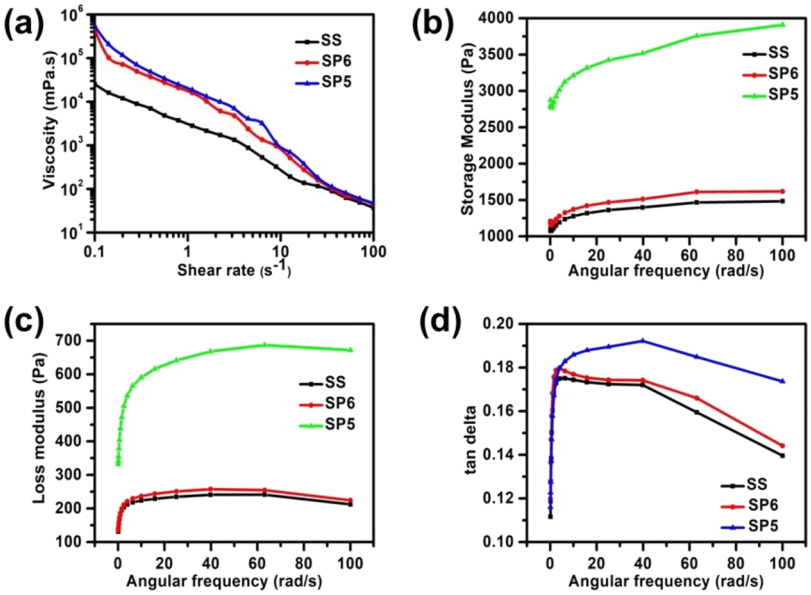

Figure 5. (a) Flow curve, (b) storage modulus, (c) loss modulus, and (d) tan δ of the hydrogels.

rheological characteristics, specifically its sensitivity to changes in viscosity based on the applied shear rate. Hydrogels typically exhibit non-Newtonian behavior, characterized by shear-thinning properties.[69] In contrast to Newtonian fluids, materials displaying shear-thinning behavior demonstrate a decrease in viscosity as the applied shear rate increases, as illustrated in Figure 5a. This property is noteworthy for hydrogels and can be advantageous in various applications, including injection, drug delivery, and tissue engineering. Figure 5a highlights that SP5 exhibits higher viscosity compared with SP6 and SS. Figure 5b,c

https://doi.org/10.1021/acsomega.4c02453
ACS Omega 2024, 9, 32706−32716

displays the curves between storage modulus (G') vs angular frequency and loss modulus (G'') vs angular frequency, respectively, to evaluate the gel strength of prepared hydrogels. The elevated storage modulus and loss modulus of SP5 compared with SP6 and SS are due to increased cross-linking within its components. The reduction in storage modulus and loss modulus observed in SP6 can likely be attributed to the emergence of a more intricate process involving chain disentanglement.[70] Figure 5d represents tan δ vs angular frequency, which highlights the fact that all of the three hydrogels have tan $\delta < 1$. This indicates that all of the three hydrogels have gel-like characteristics. Also, it can be observed from Figure 5d that SP5 has more gel-like characteristics compared with SS and SP6.[71]

3.7. Porosity. Porosity is a significant feature of hydrogels because it increases their absorption capacity, thereby increasing drug diffusion from hydrogels. Table 2 displays the porosity of prepared hydrogels, with SP5 (44.95%) having greater porosity than SP6 (14.42%). According to SEM images, SP5 possesses porous structures; however, SP6 lacks adequate blending; hence, no porous structures are observed in SP6. We observed that SP5 has interconnected components, which boost its stability and porosity. Furthermore, less porosity in SP6 is caused by a lack of interlinked components, which reduces network space and lessens the porosity.[72−74] The reduction in porosity measurement with the increase of sericin volume is due to the formation of strong cross-links, which reduces the dimension of capillary structure and interconnecting pores. The enhanced physical and chemical entanglements from the added network decrease the available network space, thereby reducing porosity.[75−77]

Table 2. Porosity of the Prepared Hydrogels

hydrogel code	porosity (%)
SP5	44.95 ± 0.11
SP6	14.42 ± 0.45

3.8. Drug Release Mechanism. From Table 1, it can be observed that stable hydrogels are formed when the volume of sericin increases but no hydrogel is formed when the volume of sericin decreases. The plausible reason might be that as the volume of sericin increases, there is a possibility of hydrogen bonding between the N−H groups of sericin and the C═O groups of polycaprolactone.[78] Moreover, the capacity of polycaprolactone to produce hydrogel decreases with an increase in its volume since it is a polyester that contains the alkoxide moiety, a poor leaving group with its negative charge entirely localized on a single oxygen atom. The plausible mechanism of the formation of SS−PCL blend hydrogels is shown in Scheme 1.

3.9. Swelling Experiments. Swelling behavior is a crucial feature of drug delivery systems, as it directly impacts the drug delivery process by influencing water absorption in hydrogels. The greater the hydrogel's water-absorbing capacity, the more drug diffusion will occur. Several factors affect swelling behavior, including the hydrogel's cross-linking density, polymer hydrophilicity, hydrophobicity, and pH. In this study, we observed the swelling nature of the prepared hydrogels (Figure 6) in distilled water and buffer solutions with different pHs. Figure 6a shows that the percentage of swelling increases over time primarily because the hydrogels encourage water diffusion and hydrogen bonding, resulting in more water absorption. SP5 exhibits the highest swelling with 62.8% at 130 min while SP6 reaches 44.9% swelling in the same time duration which is likely due to differences in aqueous stability or water interaction.[79,80] Also, from Figure 6b, it was noticed that the most significant increase in swelling occurred in the acidic medium compared with that in neutral and alkaline environments. Notably, the highest swelling was observed at pH 4 for both types of hydrogels, with SP5 (80%) demonstrating a greater swelling response than SP6 (45%). The reason might be the presence of PCL in the hydrogel network, which swells in acidic conditions.[81−83] Also, the swelling response for SP6 in both distilled water and buffer solution is less than SP5 due to the formation of strong cross-links, which restricts the entry of any fluid inside the hydrogel network.[84]

3.10. In Vitro Drug Encapsulation Efficiency. The percentage or fraction of drug loaded in the hydrogel during fabrication that is connected to the polymer network is known as drug encapsulation efficiency or DEE. It is a crucial factor to take into account when formulating hydrogels for controlled drug release systems.[85] From Figure 6c, it was observed that SP5 exhibits the highest encapsulation efficiency of 60.32%, while SP6 exhibits an encapsulation efficiency of 42.95%. This is because the drug encapsulated within the hydrogel is stabilized by hydrophobic interactions between the hydrogel's hydro-

Scheme 1. Plausible Mechanism of the Formation of SS−PCL Blend Hydrogel

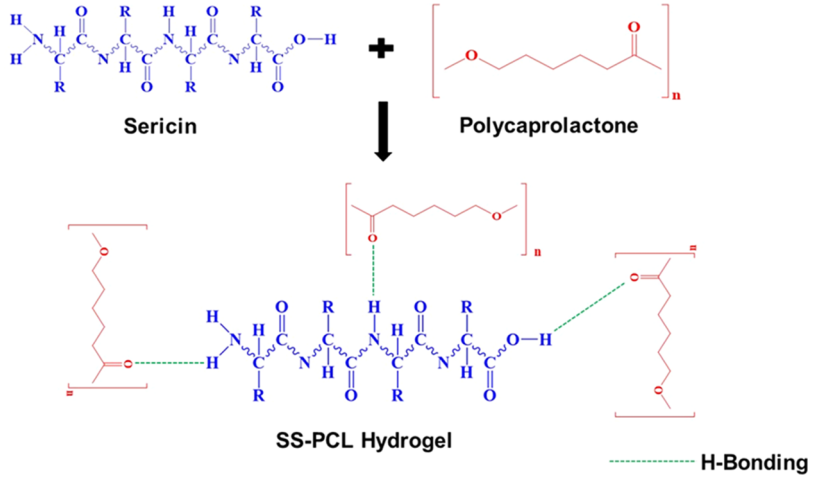

https://doi.org/10.1021/acsomega.4c02453
ACS Omega 2024, 9, 32706−32716

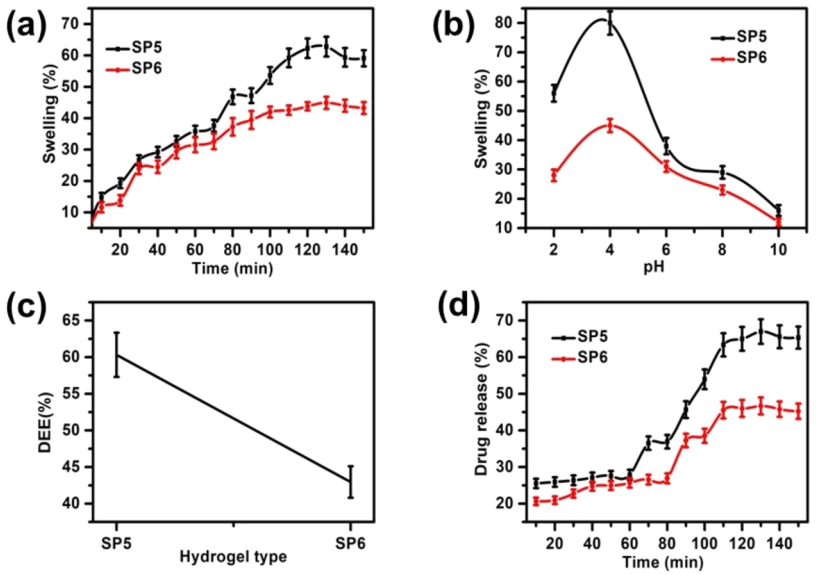

Figure 6. Swelling of the prepared hydrogels in (a) distilled water, (b) buffer solutions, (c) drug encapsulation efficiency, and (d) drug release profile of the prepared hydrogels in PBS solution (pH = 7.4).

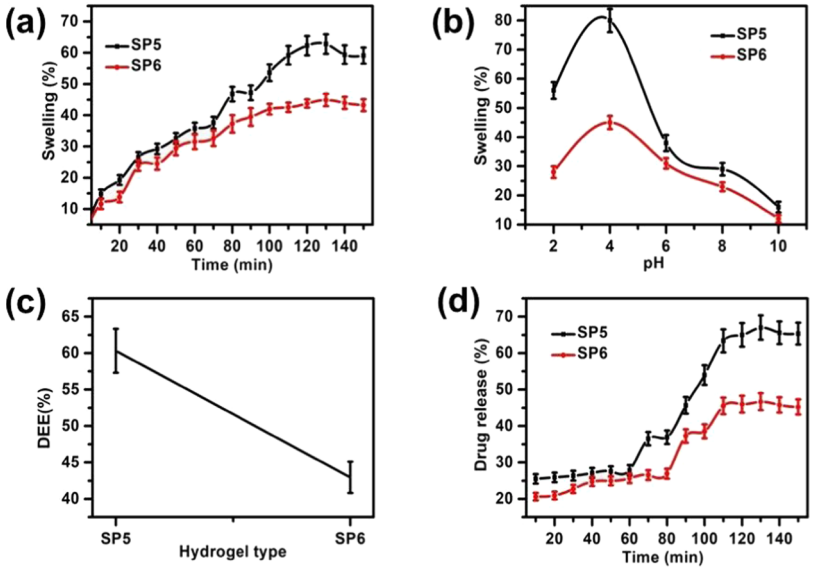

Figure 7. (a) Zero-order kinetic model, (b) pseudo-first-order kinetic model, (c) Korsmeyer−Peppas kinetic model, and (d) Higuchi kinetic model.

Table 3. Kinetic Results of the Prepared Hydrogels

hydrogel code	zero order	pseudo first order	Korsmeyer−Peppas	Higuchi
SP5	R^2 = 0.9939	R^2 = 0.9343	R^2 = 0.9687	R^2 = 0.9942
	k_o = 1.7135	k_1 = 1.5061	K = −0.6207	k_2 = 1.7057
			n = 0.1090	
SP6	R^2 = 0.9779	R^2 = 0.9092	R^2 = 0.9354	R^2 = 0.9779
	k_o = 1.6513	k_1 = 1.3068	K = −0.9131	k_2 = 1.6512
			n = 0.1683	

phobic moieties and drug molecules, ionic interactions between the drug's polar groups and the polymer chains, and hydrogen bonding between the drug molecules and the polymer network structure. Also, SP5 had a denser network structure that minimizes the possibility of leaching out the drugs from the hydrogel.[86,87]

3.11. In Vitro Drug Release Profile. When a drug permeates the hydrogel network, it undergoes diffusion along the aqueous pathway. The release of the drug is closely linked to the swelling characteristics of the hydrogel, which is a critical factor in the hydrogel design. Figure 6d depicts the time-dependent drug release from the prepared hydrogels in PBS at 37 °C. Approximately 67% of the drug was released in PBS at pH 7.4 within 130 min. Moreover, it is apparent that drug concentration also influences the release through the hydrogels, with SP5 exhibiting a higher drug release than SP6 that released

https://doi.org/10.1021/acsomega.4c02453
ACS Omega 2024, 9, 32706−32716

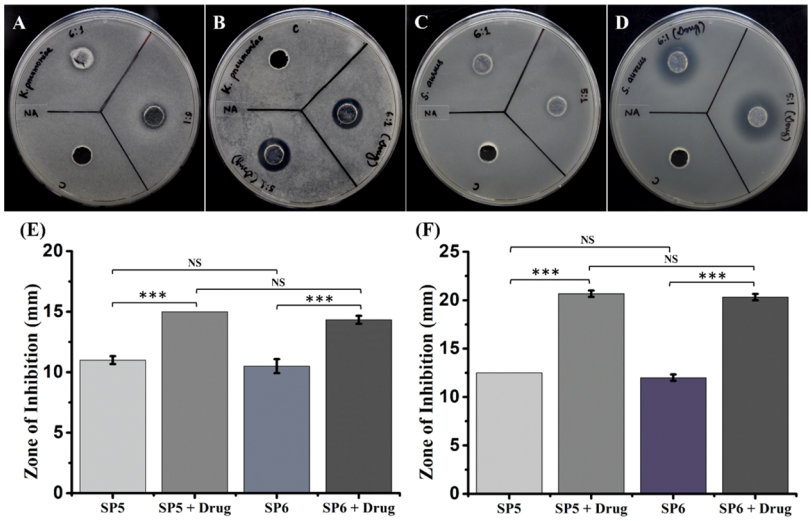

Figure 8. Petri plates showing the zones of inhibition of free (A, C) and drug-loaded (B, D) hydrogels against *K. pneumoniae* (A, B) and *S. aureus* (C, D). (E, F) The bar plot for the zone of inhibition for hydrogels. Data represent the means ± SEM of three independent experiments. Statistical differences were analyzed using one-way ANOVA. Here, *** = $P \leq 0.001$ and NS > 0.05.

Table 4. Measurement of Zones of Inhibition Created by the Prepared Hydrogels

pathogens	SP5 (mean ± SE)	SP6 (mean ± SE)	SP5 (with drug) (mean ± SE)	SP6 (with drug) (mean ± SE)
Klebsiella pneumoniae	11 ± 0.33	10.5 ± 0.58	15 ± 0	14.33 ± 0.33
Staphylococcus aureus	12.5 ± 0	12 ± 0.33	20.67 ± 0.33	20.33 ± 0.33

a drug of almost 46.68% within 130 min. These results indicate the potential of these hydrogels for use in controlled drug delivery systems.[88,89]

3.12. Drug Release Kinetics. For the kinetic study, the following plots were made: M_t vs time (zero-order kinetic model), log $(M_t - M_e)$ vs time (pseudo-first-order kinetic model), ln (M_t/M_e) vs ln(t) (Korsmeyer−Peppas kinetic model), and M_t vs $t_{1/2}$ (Higuchi model). All plots are shown in Figure 7 and the results are summarized in Table 3. From the comparison of the obtained correlation coefficients (R^2) for each kinetic model, it is understood that the release kinetics are best fitted with the zero-order kinetic model.[50] Korsmeyer−Peppas kinetic model gives the water diffusion mechanism of the prepared hydrogels. A value of $n < 0.5$ indicates Fickian diffusion phenomenon, which means that water penetration is operative. While $0.5 \leq n \leq 1$ indicates the non-Fickian diffusion, which means that the rate of polymer chain relaxation is less than penetrant velocity.[90,91] The prepared hydrogels showed a Fickian diffusion mechanism, as displayed in Table 3.

3.13. In Vitro Antibacterial Analysis. Antibacterial activities of the samples against both Gram-positive (*S. aureus*) and Gram-negative (*K. pneumoniae*) bacteria were evaluated, as shown in Figure 8 and the zone of inhibition presented in Table 4. In the absence of the hydrogels (only water), no antibacterial activity was observed, which was taken as a control. The measurement of zones of inhibition (ZOI) created by the respective hydrogels is shown in Table 4. While comparing the antibacterial effects of both the hydrogels on the pathogens *K. pneumoniae* and *S. aureus*, hydrogel SP5 was found to have slightly superior antibacterial activity with ZOI of 11 ± 0.33 and 12.5 ± 0 mm compared with hydrogel SP6 with 10.5 ± 0.58 and 12 ± 0.33 mm, respectively. However, when the hydrogels were incorporated with the DS, the antibacterial efficacy was enhanced in both the hydrogels SP5 and SP6 with ZOI 15 ± 0 and 14.33 ± 0.33 mm against *K. pneumoniae* and 20.67 ± 0.33 and 18.33 ± 0.33 mm against *S. aureus*, respectively, which is shown in Figure 8. Furthermore, it can be observed that ZOI created by drug-loaded SP5 demonstrated marginally better antibacterial efficacy compared with SP6 against both the pathogens. This might be due to the higher drug release in SP5 caused by the higher aqueous solubility of SP5.

3.14. In Vitro Biodegradation Analysis. Hydrogels possessing biodegradable qualities and retaining their structural integrity for a specified period are a preferential candidate for drug delivery applications, ensuring the controlled release of the drug at the intended location. In vitro biodegradation of the prepared hydrogels in PBS solution with respect to the time in days is shown in Figure 9. The rate of biodegradation decreases with an increase in the volume ratio of SS to PCL. A rapid decrease in biodegradation was noted within 1 day in both the hydrogels and continued for 7 days in a steady manner, with SP5 exhibiting a faster rate compared with SP6. This might be due to the greater stability and a more robust network in SP5 compared with SP6.

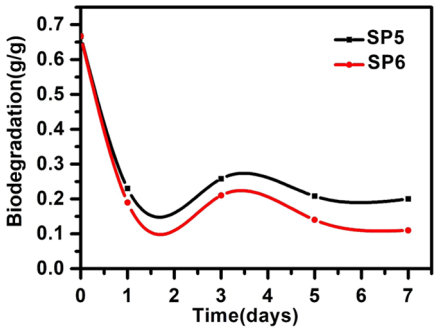

Figure 9. Biodegradation of the prepared hydrogels as a function of time (days) in PBS solution (pH = 7.4).

https://doi.org/10.1021/acsomega.4c02453
ACS Omega 2024, 9, 32706−32716

4. CONCLUSIONS

Eleven different combinations of sericin and polycaprolactone were blended to prepare hydrogels, of which the two combinations (SP5 and SP6) successfully produced stable hydrogels after incubation for 15 min. SP5 demonstrated better physicochemical properties and antibacterial activities against Gram-positive and Gram-negative bacteria than SP6. The porosity study demonstrated SP5 to be more porous (44.92%) compared with SP6 (14.42%). Further, SP5 showed a better swelling index in distilled water (62.8% in 130 min) and buffer solutions (80.0% at pH = 4) than SP6. The kinetics study proved that the drug release from the hydrogel followed the zero-order model and the Fickian diffusion model. Furthermore, both the hydrogels exhibited rapid biodegradation in 1 day and continued steadily for 7 days; however, SP5 showed better biodegradation than SP6 with higher drug release and drug encapsulation efficiency. Further investigations are required to improve the drug release efficiency of the prepared hydrogels. Furthermore, the hydrogels formed are soft and the model drug used is anti-inflammatory, hence it can be explored for transdermal drug delivery for wound healing, pain relief, and so on.

AUTHOR INFORMATION

Corresponding Author

Kamatchi Sankaranarayanan − *Institute of Advanced Study in Science and Technology (An Autonomous Institute Under DST, Govt. of India), Guwahati 781035 Assam, India; Academy of Scientific and Innovative Research (AcSIR), Ghaziabad 201002, India;* orcid.org/0000-0002-2742-1994; Email: kamatchi.sankaran@gmail.com

Authors

Dona Deb − *Institute of Advanced Study in Science and Technology (An Autonomous Institute Under DST, Govt. of India), Guwahati 781035 Assam, India; Academy of Scientific and Innovative Research (AcSIR), Ghaziabad 201002, India*

Bably Khatun − *Institute of Advanced Study in Science and Technology (An Autonomous Institute Under DST, Govt. of India), Guwahati 781035 Assam, India*

Bidyarani Devi M − *Institute of Advanced Study in Science and Technology (An Autonomous Institute Under DST, Govt. of India), Guwahati 781035 Assam, India*

Mojibur R. Khan − *Institute of Advanced Study in Science and Technology (An Autonomous Institute Under DST, Govt. of India), Guwahati 781035 Assam, India*

Neelotpal Sen Sarma − *Institute of Advanced Study in Science and Technology (An Autonomous Institute Under DST, Govt. of India), Guwahati 781035 Assam, India;* orcid.org/0000-0002-2666-6316

Complete contact information is available at: https://pubs.acs.org/10.1021/acsomega.4c02453

Author Contributions

§D.D. and B.K. contributed equally to this work.

Notes

The authors declare no competing financial interest.

ACKNOWLEDGMENTS

This work was supported by the ICMR Project grant (File No. 17x (3)/Ad-hoc/19/2022-ITR dt. 23.12.2022), DST-IASST, Guwahati In-house project grant, and SRG grant (SRG/2020/001894 dt. 11.11.2020). The authors thank SAIC, IASST, for the instrumentation facilities.

REFERENCES

(1) Tabakoglu, S.; Kołbuk, D.; Sajkiewicz, P. Multifluid electrospinning for multi-drug delivery systems: Pros and cons, challenges, and future directions. *Biomater. Sci.* **2022**, *11*, 37−61.

(2) Hardenia, A.; Maheshwari, N.; Hardenia, S. S.; Dwivedi, S. K.; Maheshwari, R.; Tekade, R. K.Scientific Rationale for Designing Controlled Drug Delivery Systems. In *Basic Fundamentals of Drug Delivery*; Elsevier, 2019; pp 1−28. DOI: 10.1016/B978-0-12-817909-3.00001-7.

(3) Kamaly, N.; Yameen, B.; Wu, J.; Farokhzad, O. C. Degradable controlled-release polymers and polymeric nanoparticles: mechanisms of controlling drug release. *Chem. Rev.* **2016**, *116*, 2602−2663.

(4) Huang, D.; Sun, M.; Bu, Y.; Luo, F.; Lin, C.; Lin, Z.; Weng, Z.; Yang, F.; Wu, D. Microcapsule-embedded hydrogel patches for ultrasound responsive and enhanced transdermal delivery of diclofenac sodium. *J. Mater. Chem. B* **2019**, *7*, 2330−2337.

(5) Anwar, F.; Amin, K. F.; Hoque, M. E.Tools and techniques for characterizing sustainable hydrogels. In *Sustainable Hydrogels*; Elsevier, 2023; pp 47−77.

(6) Khan, F.; Atif, M.; Haseen, M.; Kamal, S.; Khan, M. S.; Shahid, S.; Nami, S. A. Synthesis, classification and properties of hydrogels: Their applications in drug delivery and agriculture. *J. Mater. Chem. B* **2022**, *10*, 170−203.

(7) Ye, B.; Wu, B.; Su, Y.; Sun, T.; Guo, X. Recent advances in the application of natural and synthetic polymer-based scaffolds in musculoskeletal regeneration. *Polymers* **2022**, *14*, 4566.

(8) Dubey, P.; Seit, S.; Chowdhury, P. K.; Ghosh, S. Effect of Macromolecular Crowders on the Self-Assembly Process of Silk Fibroin. *Macromol. Chem. Phys.* **2020**, *221*, No. 2000113.

(9) Ode Boni, B. O.; Bakadia, B. M.; Osi, A. R.; Shi, Z.; Chen, H.; Gauthier, M.; Yang, G. Immune response to silk sericin−fibroin composites: potential immunogenic elements and alternatives for immunomodulation. *Macromol. Biosci.* **2022**, *22*, No. 2100292.

(10) Reddy, M. S. B.; Ponnamma, D.; Choudhary, R.; Sadasivuni, K. K. A comparative review of natural and synthetic biopolymer composite scaffolds. *Polymers* **2021**, *13*, No. 1105.

(11) Biswal, B.; Dan, A. K.; Sengupta, A.; Das, M.; Bindhani, B. K.; Das, D.; Parhi, P. K. Extraction of silk fibroin with several sericin removal processes and its importance in tissue engineering: A review. *J. Polym. Environ.* **2022**, *30*, 2222−2253.

(12) Jaramillo-Quiceno, N.; Callone, E.; Dirè, S.; Álvarez-López, C.; Motta, A. Boosting sericin extraction through alternative silk sources. *Polym. J.* **2021**, *53*, 1425−1437.

(13) Rajasekaran, R.; Seesala, V. S.; Sunka, K. C.; Ray, P. G.; Saha, B.; Banerjee, M.; Dhara, S. Role of nanofibers on MSCs fate: Influence of fiber morphologies, compositions and external stimuli. *Mater. Sci. Eng.: C* **2020**, *107*, No. 110218.

(14) El-Samad, L. M.; Hassan, M. A.; Basha, A. A.; El-Ashram, S.; Radwan, E. H.; Aziz, K. K. A.; Tamer, T. M.; Augustyniak, M.; El Wakil, A. Carboxymethyl cellulose/sericin-based hydrogels with intrinsic antibacterial, antioxidant, and anti-inflammatory properties promote re-epithelization of diabetic wounds in rats. *Int. J. Pharm.* **2022**, *629*, No. 122328.

(15) Ma, Y.; Tong, X.; Huang, Y.; Zhou, X.; Yang, C.; Chen, J.; Dai, F.; Xiao, B. Oral administration of hydrogel-embedding silk sericin alleviates ulcerative colitis through wound healing, anti-inflammation, and anti-oxidation. *ACS Biomater. Sci. Eng.* **2019**, *5*, 6231−6242.

(16) Munir, F.; Tahir, H. M.; Ali, S.; Ali, A.; Tehreem, A.; Zaidi, S. D. E. S.; Adnan, M.; Ijaz, F. Characterization and Evaluation of Silk Sericin-Based Hydrogel: A Promising Biomaterial for Efficient Healing of Acute Wounds. *ACS Omega* **2023**, *8*, 32090−32098.

(17) Balcão, V. M.; Harada, L. K.; Jorge, L. R.; Oliveira, J. M., Jr; Tubino, M.; Vila, M. M. Structural and functional stabilization of sericin from Bombyx mori cocoons in a biopolysaccharide film: Bioorigami for skin regeneration. *J. Braz. Chem. Soc.* **2020**, *31*, 833−848.

(18) Zhang, Y.; Zhao, Y.; He, X.; Fang, A.; Jiang, R.; Wu, T.; Chen, H.; Cao, X.; Liang, P.; Xia, D.; Zhang, G. A sterile self-assembled sericin hydrogel via a simple two-step process. *Polym. Test.* **2019**, *80*, No. 106016.
(19) Al-Tabakha, M. M.; Khan, S. A.; Ashames, A.; Ullah, H.; Ullah, K.; Murtaza, G.; Hassan, N. Synthesis, characterization and safety evaluation of sericin-based hydrogels for controlled delivery of acyclovir. *Pharmaceuticals* **2021**, *14*, 234.
(20) Al-Baadani, M. A.; Yie, K. H. R.; Al-Bishari, A. M.; Alshobi, B. A.; Zhou, Z.; Fang, K.; Dai, B.; Shen, Y.; Ma, J.; Liu, J.; Shen, X. Co-electrospinning polycaprolactone/gelatin membrane as a tunable drug delivery system for bone tissue regeneration. *Mater. Des.* **2021**, *209*, No. 109962.
(21) Ahmad, Z.; Salman, S.; Khan, S. A.; Amin, A.; Rahman, Z. U.; Al-Ghamdi, Y. O.; Akhtar, K.; Bakhsh, E. M.; Khan, S. B. Versatility of hydrogels: from synthetic strategies, classification, and properties to biomedical applications. *Gels* **2022**, *8*, 167.
(22) Verma, Y.; Sharma, G.; Kumar, A.; Dhiman, P.; Si, C.; an Stadler, F. J. Synthesizing pectin-crosslinked gum ghatti hydrogel for efficient adsorptive removal of malachite green. *Int. J. Biol. Macromol.* **2024**, *258*, No. 128640.
(23) Gull, N.; Khan, S. M.; Butt, O. M.; Islam, A.; Shah, A.; Jabeen, S.; Khan, S. U.; Khan, A.; Khan, R. U.; Butt, M. T. Z. Inflammation targeted chitosan-based hydrogel for controlled release of diclofenac sodium. *Int. J. Biol. Macromol.* **2020**, *162*, 175−187.
(24) Constantino, V. R. L.; Figueiredo, M. P.; Magri, V. R.; Eulálio, D.; Cunha, V. R. R.; Alcântara, A. C. S.; Perotti, G. F. Biomaterials based on organic polymers and layered double hydroxides nanocomposites: Drug delivery and tissue engineering. *Pharmaceutics* **2023**, *15*, 413.
(25) Malikmammadov, E.; Tanir, T. E.; Kiziltay, A.; Hasirci, V.; Hasirci, N. PCL and PCL-based materials in biomedical applications. *J. Biomater. Sci., Polym. Ed.* **2018**, *29*, 863−893.
(26) Perera, W. P. T. D.; Dissanayake, D. R. K.; Unagolla, J. M.; De Silva, R. T.; Bathige, S. D.; Pahalagedara, L. R. Albumin grafted coaxial electrosparyed polycaprolactone-zinc oxide nanoparticle for sustained release and activity enhanced antibacterial drug delivery. *RSC Adv.* **2022**, *12*, 1718−1727.
(27) Tao, G.; Cai, R.; Wang, Y.; Liu, L.; Zuo, H.; Zhao, P.; Umar, A.; Mao, C.; Xia, Q.; He, H. Bioinspired design of AgNPs embedded silk sericin-based sponges for efficiently combating bacteria and promoting wound healing. *Mater. Des.* **2019**, *180*, No. 107940.
(28) Zhao, R.; Li, X.; Sun, B.; Tong, Y.; Jiang, Z.; Wang, C. Nitrofurazone-loaded electrospun PLLA/sericin-based dual-layer fiber mats for wound dressing applications. *RSC Adv.* **2015**, *5*, 16940−16949.
(29) Ekasurya, W.; Sebastian, J.; Puspitasari, D.; Asri, P. P.; Asri, L. A. Synthesis and degradation properties of sericin/PVA hydrogels. *Gels* **2023**, *9*, 76.
(30) Tuancharoensri, N.; Sonjan, S.; Promkrainit, S.; Daengmankhong, J.; Phimnuan, P.; Mahasaranon, S.; Jongjitwimol, J.; Charoensit, P.; Ross, G. M.; Viennet, C.; Viyoch, J. Porous Poly (2-hydroxyethyl methacrylate) Hydrogel Scaffolds for Tissue Engineering: Influence of Crosslinking Systems and Silk Sericin Concentration on Scaffold Properties. *Polymers* **2023**, *15*, No. 4052.
(31) Fazal, T.; Murtaza, B. N.; Shah, M.; Iqbal, S.; Rehman, M. U.; Jaber, F.; Dera, A. A.; Awwad, N. S.; Ibrahium, H. A. Recent developments in natural biopolymer based drug delivery systems. *RSC Adv.* **2023**, *13*, 23087−23121.
(32) Fouad, S. A.; Basalious, E. B.; El-Nabarawi, M. A.; Tayel, S. A. Microemulsion and poloxamer microemulsion-based gel for sustained transdermal delivery of diclofenac epolamine using in-skin drug depot: in vitro/in vivo evaluation. *Int. J. Pharm.* **2013**, *453*, 569−578.
(33) Kaliaraj, G. S.; Shanmugam, D. K.; Dasan, A.; Mosas, K. K. A. Hydrogels−A Promising Materials for 3D Printing Technology. *Gels* **2023**, *9*, 260.
(34) Risbud, M. V.; Bhat, S. V. Properties of polyvinyl pyrrolidone/β-chitosan hydrogel membranes and their biocompatibility evaluation by haemorheological method. *J. Mater. Sci.: Mater. Med.* **2001**, *12*, 75−79.
(35) Kamath, S. M.; Sridhar, K.; Jaison, D.; Gopinath, V.; Ibrahim, B. M.; Gupta, N.; Sundaram, A.; Sivaperumal, P.; Padmapriya, S.; Patil, S. S. Fabrication of tri-layered electrospun polycaprolactone mats with improved sustained drug release profile. *Sci. Rep.* **2020**, *10*, No. 18179.
(36) Dave, P. N.; Macwan, P. M.; Kamaliya, B. Biodegradable Gg-cl-poly (NIPAm-co-AA)/-o- MWCNT based hydrogel for combined drug delivery system of metformin and sodium diclofenac: in vitro studies. *RSC Adv.* **2023**, *13*, 22875−22885.
(37) Nikolova, D.; Simeonov, M.; Tzachev, C.; Apostolov, A.; Christov, L.; Vassileva, E. Polyelectrolyte complexes of chitosan and sodium alginate as a drug delivery system for diclofenac sodium. *Polym. Int.* **2022**, *71*, 668−678.
(38) Tan, L. S.; Tan, H. L.; Deekonda, K.; Wong, Y. Y.; Muniyandy, S.; Hashim, K.; Pushpamalar, J. Fabrication of radiation cross-linked diclofenac sodium loaded carboxymethyl sago pulp/chitosan hydrogel for enteric and sustained drug delivery. *Carbohydr. Polym. Technol. Appl.* **2021**, *2*, No. 100084.
(39) Kalita, M.; Allardyce, B. J.; Sankaranarayanan, K.; Devi, D.; Rajkhowa, R. Sericin from mulberry and non-mulberry silk using chemical-free degumming. *J. Text. Inst.* **2022**, *113*, 2080−2089.
(40) Kalita, M.; Sarma, C.; Kalita, M.; Sarmah, V.; Sankaranarayanan, K. Efficient Extraction of Sericin Protein from Mulberry and Non-Mulberry Silk Fibers: Utilizing Aqueous Ionic Liquid Solutions as Green Solvents. *ChemistrySelect* **2024**, *9*, No. 202304064.
(41) Cwiertnia, B. Effect of water soluble carrier on dissolution profiles of diclofenac sodium. *Acta Polym. Pharm.* **2013**, *70*, 721−726.
(42) Saei, A. A.; Jabbaribar, F.; Fakhree, M. A. A.; Acree, W. E., Jr.; Jouyban, A. Solubility of sodium diclofenac in binary water+ alcohol solvent mixtures at 25 °C. *J. Drug Delivery Sci. Technol.* **2008**, *18*, 149−151.
(43) Žilnik, L. F.; Jazbinšek, A.; Hvala, A.; Vrečer, F.; Klamt, A. Solubility of sodium diclofenac in different solvents. *Fluid Phase Equilib.* **2007**, *261*, 140−145.
(44) Calverley, J.; Zimmerman, W. B.; Leak, D. J.; Bandulasena, H. H. Continuous removal of ethanol from dilute ethanol-water mixtures using hot microbubbles. *Chem. Eng. J.* **2021**, *424*, No. 130511.
(45) Lan, Z.; Kar, R.; Chwatko, M.; Shoga, E.; Cosgriff-Hernandez, E. High porosity PEG-based hydrogel foams with self-tuning moisture balance as chronic wound dressings. *J. Biomed. Mater. Res., Part A* **2023**, *111*, 465−477.
(46) Cui, L.; Wu, F.; Wang, W.; Hu, C.; Zheng, J.; Zhu, Z.; Liu, B. Robust and Elastic Thermoresponsive Hydrogels with High Swelling Properties for Efficient Solar Water Purification. *ACS Appl. Polym. Mater.* **2024**, *6*, 3253−3262.
(47) Pande, S. Liposomes for drug delivery: review of vesicular composition, factors affecting drug release and drug loading in liposomes. *Artif. Cells, Nanomed., Biotechnol.* **2023**, *51*, 428−440.
(48) Sreedharan, S. M.; Singh, R. Ciprofloxacin functionalized biogenic gold nanoflowers as nanoantibiotics against pathogenic bacterial strains. *Int. J. Nanomed.* **2019**, *14*, 9905−9916.
(49) Abbas, A.; Hussain, M. A.; Amin, M.; Tahir, M. N.; Jantan, I.; Hameed, A.; Bukhari, S. N. A. Multiple cross-linked hydroxypropyl-cellulose−succinate−salicylate: prodrug design, characterization, stimuli responsive swelling−deswelling and sustained drug release. *RSC Adv.* **2015**, *5*, 43440−43448.
(50) Pathania, D.; Verma, C.; Negi, P.; Tyagi, I.; Asif, M.; Kumar, N. S.; Al-Ghurabi, E. H.; Agarwal, S.; Gupta, V. K. Novel nanohydrogel based on itaconic acid grafted tragacanth gum for controlled release of ampicillin. *Carbohydr. Polym.* **2018**, *196*, 262−271.
(51) Samuelov, Y.; Donbrow, M.; Friedman, M. Sustained release of drugs from ethylcellulose-polyethylene glycol films and kinetics of drug release. *J. Pharm. Sci.* **1979**, *68*, 325−329.
(52) Chen, C. C.; Lai, C. C.; Toh, H. S.; Tang, H. J. Antimicrobial activity of Lactobacillus species against carbapenem-resistant Enterobacteriaceae. *Front. Microbiol.* **2019**, *10*, No. 789.
(53) Humphries, R.; Bobenchik, A. M.; Hindler, J. A.; Schuetz, A. N. Overview of changes to the clinical and laboratory standards institute performance standards for antimicrobial susceptibility testing, M100. *J. Clin. Microbiol.* **2021**, *59*, No. e0021321.

https://doi.org/10.1021/acsomega.4c02453
ACS Omega 2024, 9, 32706−32716

(54) Tanan, W.; Panichpakdee, J.; Saengsuwan, S. Novel biodegradable hydrogel based on natural polymers: Synthesis, characterization, swelling/reswelling and biodegradability. *Eur. Polym. J.* **2019**, *112*, 678−687.
(55) Kwon, S. S.; Kong, B. J.; Park, S. N. Physicochemical properties of pH-sensitive hydrogels based on hydroxyethyl cellulose−hyaluronic acid and for applications as transdermal delivery systems for skin lesions. *Eur. J. Pharm. Biopharm.* **2015**, *92*, 146−154.
(56) Ali, S. M.; Yosipovitch, G. Skin pH: from basic science to basic skin care. *Acta Derm.-Venereol.* **2013**, *93*, 261−267.
(57) Mauro, T.; Grayson, S.; Gao, W. N.; Man, M. Q.; Kriehuber, E.; Behne, M.; Feingold, K. R.; Elias, P. M. Barrier recovery is impeded at neutral pH, independent of ionic effects: implications for extracellular lipid processing. *Arch. Dermatol. Res.* **1998**, *290*, 215−222.
(58) Sabbagh, F.; Kim, B. S. Recent advances in polymeric transdermal drug delivery systems. *J. Controlled Release* **2022**, *341*, 132−146.
(59) Akombaetwa, N.; Ilangala, A. B.; Thom, L.; Memvanga, P. B.; Witika, B. A.; Buya, A. B. Current advances in lipid nanosystems intended for topical and transdermal drug delivery applications. *Pharmaceutics* **2023**, *15*, 656.
(60) Purcea Lopes, P. M.; Moldovan, D.; Fechete, R.; Mare, L.; Barbu-Tudoran, L.; Sechel, N.; Popescu, V. Characterization of a Graphene Oxide-Reinforced Whey Hydrogel as an Eco-Friendly Absorbent for Food Packaging. *Gels* **2023**, *9*, 298.
(61) Zhang, H.; Li, L. L.; Dai, F. Y.; Zhang, H. H.; Ni, B.; Zhou, W.; Yang, X.; Wu, Y. Z. Preparation and characterization of silk fibroin as a biomaterial with potential for drug delivery. *J. Transl. Med.* **2012**, *10*, No. 117.
(62) Rehman, I.; Farooq, M.; Botelho, S. Biochemistry, secondary protein structure. 2017.
(63) Teramoto, H.; Miyazawa, M. Analysis of structural properties and formation of sericin fiber by infrared spectroscopy. *J. Insect Biotechnol. Sericol.* **2003**, *72*, 157−162.
(64) Liu, J.; Qi, C.; Tao, K.; Zhang, J.; Zhang, J.; Xu, L.; Jiang, X.; Zhang, Y.; Huang, L.; Li, Q.; Xie, H. Sericin/dextran injectable hydrogel as an optically trackable drug delivery system for malignant melanoma treatment. *ACS Appl. Mater. Interfaces* **2016**, *8*, 6411−6422.
(65) Cai, S.; Singh, B. R. Identification of β-turn and random coil amide III infrared bands for secondary structure estimation of proteins. *Biophys. Chem.* **1999**, *80*, 7−20.
(66) Martínez, D. C. C.; Zuluaga, C. L.; Restrepo-Osorio, A.; Álvarez-López, C. Characterization of sericin obtained from cocoons and silk yarns. *Procedia Eng.* **2017**, *200*, 377−383.
(67) Kumar, S.; Koh, J. Physiochemical, optical and biological activity of chitosan-chromone derivative for biomedical applications. *Int. J. Mol. Sci.* **2012**, *13*, 6102−6116.
(68) Voronova, M.; Rubleva, N.; Kochkina, N.; Afineevskii, A.; Zakharov, A.; Surov, O. Preparation and characterization of polyvinylpyrrolidone/cellulose nanocrystals composites. *Nanomaterials* **2018**, *8*, 1011.
(69) Latifi, N.; Asgari, M.; Vali, H.; Mongeau, L. A tissue-mimetic nano-fibrillar hybrid injectable hydrogel for potential soft tissue engineering applications. *Sci. Rep.* **2018**, *8*, No. 1047.
(70) Gong, J.; Wang, L.; Wu, J.; Yuan, Y.; Mu, R. J.; Du, Y.; Wu, C.; Pang, J. The rheological and physicochemical properties of a novel thermosensitive hydrogel based on konjac glucomannan/gum tragacanth. *LWT* **2019**, *100*, 271−277.
(71) Stojkov, G.; Niyazov, Z.; Picchioni, F.; Bose, R. K. Relationship between structure and rheology of hydrogels for various applications. *Gels* **2021**, *7*, 255.
(72) Pan, H.; Fan, D.; Duan, Z.; Zhu, C.; Fu, R.; Li, X. Non-stick hemostasis hydrogels as dressings with bacterial barrier activity for cutaneous wound healing. *Mater. Sci. Eng.: C* **2019**, *105*, No. 110118.
(73) Lv, F.; Wang, C.; Zhu, P.; Zhang, C. Characterization of chitosan microparticles reinforced cellulose biocomposite sponges regenerated from ionic liquid. *Cellulose* **2014**, *21*, 4405−4418.
(74) Bukhari, S. M. H.; Khan, S.; Rehanullah, M.; Ranjha, N. M. Synthesis and characterization of chemically cross-linked acrylic acid/gelatin hydrogels: effect of pH and composition on swelling and drug release. *Int. J. Polym. Sci.* **2015**, *2015*, No. 187961.
(75) Yin, J.; Huang, G.; Chen, X.; Shen, J.; An, C.; Chen, N.; Feng, R.; Rosendahl, S. Recyclable sericin/nanocellulose aerogel with high adsorption capacity for tetrabromobisphenol A in water: Insight from DFT calculations. *Chem. Eng. J.* **2023**, *474*, No. 145695.
(76) Walker, B. W.; Lara, R. P.; Mogadam, E.; Yu, C. H.; Kimball, W.; Annabi, N. Rational design of microfabricated electroconductive hydrogels for biomedical applications. *Prog. Polym. Sci.* **2019**, *92*, 135−157.
(77) Zhang, L.; Ma, W.; Tang, H.; Yu, Y.; Wang, L.; Li, T.; Fang, Z.; Qiao, Z. Tough, low-friction and homogeneous physical hydrogel by a solvent-inducted strategy. *Chem. Eng. J.* **2023**, *466*, No. 143195.
(78) Matta, C. F.; Hernández-Trujillo, J.; Tang, T. H.; Bader, R. F. Hydrogen−hydrogen bonding: a stabilizing interaction in molecules and crystals. *Chem. - Eur. J.* **2003**, *9*, 1940−1951.
(79) Sizílio, R. H.; Galvão, J. G.; Trindade, G. G. G.; Pina, L. T. S.; Andrade, L. N.; Gonsalves, J. K. M. C.; Lira, A. A. M.; Chaud, M. V.; Alves, T. F. R.; Arguelho, M. L. P. M.; Nunes, R. S. Chitosan/pvp-based mucoadhesive membranes as a promising delivery system of betamethasone-17-valerate for aphthous stomatitis. *Carbohydr. Polym.* **2018**, *190*, 339−345.
(80) Khatun, B.; Rather, M. A.; Rohilla, S.; Borah, R.; Mandal, M.; Maji, T. K. Curcumin−hydroxypropyl-β-cyclodextrin complex preparation methods: a comparative study. *Chem. Pap.* **2023**, *77*, 4409−4424.
(81) Zhao, L.; Xu, L.; Mitomo, H.; Yoshii, F. Synthesis of pH-sensitive PVP/CM-chitosan hydrogels with improved surface property by irradiation. *Carbohydr. Polym.* **2006**, *64*, 473−480.
(82) Bardajee, G. R.; Mahmoodian, H.; Boraghi, S. A.; Elmizadeh, H.; Ziarani, N. B.; Rezanejad, Z.; Tyagi, I.; Gaur, R.; Javadian, H. Nanoporous hydrogel absorbent based on salep: Swelling behavior and methyl orange adsorption capacity. *Environ. Res.* **2023**, *225*, No. 115571.
(83) Marsano, E.; Bianchi, E.; Vicini, S.; Compagnino, L.; Sionkowska, A.; Skopińska, J.; Wiśniewski, M. Stimuli responsive gels based on interpenetrating network of chitosan and poly (vinylpyrrolidone). *Polymer* **2005**, *46*, 1595−1600.
(84) Kim, A.; Mujumdar, S. K.; Siegel, R. A. Swelling properties of hydrogels containing phenylboronic acids. *Chemosensors* **2014**, *2*, 1−12.
(85) Wallace, S. J.; Li, J.; Nation, R. L.; Boyd, B. J. Drug release from nanomedicines: selection of appropriate encapsulation and release methodology. *Drug Delivery Transl. Res.* **2012**, *2*, 284−292.
(86) Maswal, M.; Chat, O. A.; Dar, A. A. Rheological characterization of multi-component hydrogel based on carboxymethyl cellulose: insight into its encapsulation capacity and release kinetics towards ibuprofen. *Colloid Polym. Sci.* **2015**, *293*, 1723−1735.
(87) Banerjee, S.; Chaurasia, G.; Pal, D.; Ghosh, A. K.; Ghosh, A.; Kaity, S. Investigation on crosslinking density for development of novel interpenetrating polymer network (IPN) based formulation. *J. Sci. Ind. Res.* **2010**, *69*, 777−784.
(88) Khurma, J. R.; Nand, A. V. Temperature and pH sensitive hydrogels composed of chitosan and poly (ethylene glycol). *Polym. Bull.* **2008**, *59*, 805−812.
(89) Lin, W. C.; Yu, D. G.; Yang, M. C. pH-sensitive polyelectrolyte complex gel microspheres composed of chitosan/sodium tripolyphosphate/dextran sulfate: swelling kinetics and drug delivery properties. *Colloids Surf., B* **2005**, *44*, 143−151.
(90) Anirudhan, T. S.; Rejeena, S. R. Poly (acrylic acid-co-acrylamide-co-2-acrylamido-2-methyl-1-propanesulfonic acid) -grafted nanocellulose/poly (vinyl alcohol) composite for the in vitro gastrointestinal release of amoxicillin. *J. Appl. Polym. Sci.* **2014**, *131* (17), No. 40699.
(91) Sarmah, D.; Rather, M. A.; Sarkar, A.; Mandal, M.; Sankaranarayanan, K.; Karak, N. Self-cross-linked starch/chitosan hydrogel as a biocompatible vehicle for controlled release of drug. *Int. J. Biol. Macromol.* **2023**, *237*, No. 124206.

https://doi.org/10.1021/acsomega.4c02453
ACS Omega 2024, 9, 32706−32716